PERGAMON

Available online at www.sciencedirect.com
SCIENCE DIRECT®

Chaos, Solitons and Fractals 18 (2003) 149–158

CHAOS
SOLITONS & FRACTALS

www.elsevier.com/locate/chaos

An inductorless CMOS realization of Chua's circuit

Ahmed G. Radwan *, Ahmed M. Soliman, Abdel-Latif El-Sedeek

Faculty of Engineering, Cairo University, Egypt

Accepted 19 November 2002

Abstract

In this paper, an inductorless CMOS realization of Chua's circuit [IEEE Trans. Circ. Syst.—I 1985;32:798] is presented. The circuit is derived from the dimensionless form of Chua's circuit and can generate Rossler or double-scroll attractors by changing a single capacitor's value. Variables are represented in the current domain to facilitate adding or subtracting variables. New G_m–C representation of the Chua diode as well as the Chua circuit are presented. The circuit can operate from supply voltage as low as ±1.5 V. Transistor-level simulation results using PSpice in 0.5 μm Mietec process are presented.

1. Introduction

The great expectations promised by research in chaotic electronic circuits has been proved during the last few decades through its wide applications such as signal encryption and secure communications [2–5]. The design of chaotic circuits is a very rich subject showing different approaches [3–9]. One of these approaches is the redesign of already existing circuits to facilitate its utilization in industry. Chua's circuits are considered one of the most famous circuits existing until now. The circuits are composed of a network of linear passive elements (resistors, capacitors and inductor) connected to a nonlinear active component called Chua's diode. One of the famous Chua's circuits is shown in Fig. 1(a) which can be described by the following set of equations:

$$\begin{aligned} C_1\frac{dV_1}{dt} &= \frac{V_2}{R} - I_N \\ C_2\frac{dV_2}{dt} &= I_3 + \frac{V_1 - V_2}{R} \\ \frac{dI_3}{dt} &= -\frac{V_2}{L} \end{aligned} \tag{1}$$

where I_N is the current in the voltage-controlled nonlinear resistor which is modeled by

$$I_N = G_b V_1 + \tfrac{1}{2}(G_a - G_b)(|V_1 + V_B| - |V_1 - V_B|) \tag{2}$$

These above equation describes Chua's diode which is a three segment piece wise linear function with G_a and G_b as the slopes of the I–V characteristic in the inner and outer segments, respectively and $\pm V_B$ are the breakpoints as shown in Fig. 1(b).

This circuit is rich in behavior which made it very popular through its ability of producing different attractors such as Rossler attractor and double-scroll attractor [1,2]. But unfortunately, at the frequency ranges of interest, the above inductor cannot be integrated which led researchers to replace the inductor by equivalent circuits using large block diagrams such as Op-amps [6,7] that showed the problems of consuming high power supply and large die area. From

* Corresponding author.

0960-0779/03/$ - see front matter © 2003 Published by Elsevier Science Ltd.
doi:10.1016/S0960-0779(02)00582-9

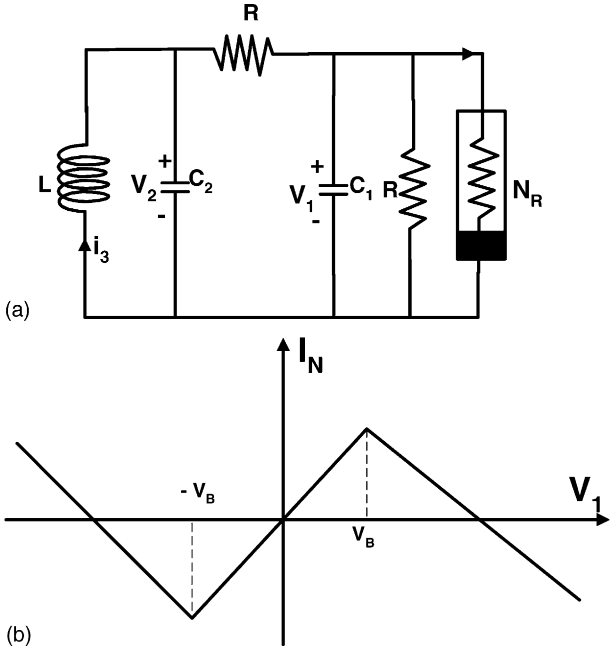

Fig. 1. (a) Chua's circuit and (b) I_N–V_1 characteristic of Chua's diode.

another prospective, the design of Chua's diode is also usually implemented using Op-amps [8]. Further researches suggested that Chua's circuit can be decomposed into two parts a sinusoidal oscillator coupled to Chua's diode [9] which also required the use of large block diagrams. An additional approach was designing a new circuit that has the same dimensionless form (looking at Chua's circuit as a single block diagram). The dimensionless form of Chua's circuit presented by Eqs. (1) and (2) becomes [2]

$$\begin{aligned} \dot{X} &= \alpha(Y - f(X)) \\ \dot{Y} &= Z + X - Y \\ \dot{Z} &= -\beta Y \end{aligned} \tag{3}$$

$$f(X) = \left\{ \begin{array}{ll} m_1X + (m_1 - m_0) & X < -1 \\ m_0X & -1 < X < 1 \\ m_1X - (m_1 - m_0) & 1 < X \end{array} \right\} \tag{4}$$

where α and β are constant parameters.

The current mode techniques may be used as a means of realizing these equations as presented by the circuit in [3]. However, this circuit dealt with differential pairs biased by different current sources for both Chua's diode and Chua's circuit which operate from ±2.5 V, consume power and are difficult to control.

This paper uses the dimensionless form of Chua's circuit in a way that is most suitable for current mode realization operating from supply voltages as low as ±1.5 V. Therefore this realization is expected to occupy less die area and consume less power than other realizations found in the literature [1–9]. Also a new realization of Chua's diode is presented based on simple G_m which makes it easier to control the breakpoints.

This paper is organized as follows: in the next section the transformation to voltage-based form then into a set of equations that are easier to implement using G_m–C integrators. In Section 3, the implementation of Chua's diode and the complete Chua's circuit are discussed. The simulation results are given in Section 4.

2. Synthesis using current integrators

The dimensionless form in Eqs. (3) and (4) have all the characteristics of Chua's circuit, so, we can retransform this dimensionless form into voltage-mode differential equations which results in inductorless realization. Hence through the dimensionless quantities

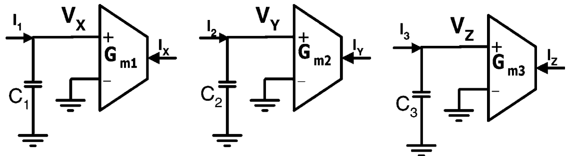

Fig. 2. Three simple current integrators.

$$X = \frac{V_X}{V_R}, \quad Y = \frac{V_Y}{V_R}, \quad Z = \frac{V_Z}{V_R}, \quad \tau = \frac{g_m t}{C}$$

where g_m is the transconductance, C is a capacitance and V_R is a reference voltage. When we apply the above transformation to the dimensionless form we get the voltage-based differential equations as follows:

$$\begin{aligned} C\dot{V}_X &= \alpha(g_m V_Y - f(V_X)) \\ C\dot{V}_Y &= g_m(V_X - V_Y + V_Z) \\ C\dot{V}_Z &= -\beta g_m V_Y \end{aligned} \tag{5}$$

$$f(V_X) = \begin{cases} r_1 V_X + (r_1 - r_0)V_R, & V_X \leqslant -V_R \\ r_0 V_X, & -V_R < V_X < V_R \\ r_1 V_X - (r_1 - r_0)V_R, & V_R \leqslant V_X \end{cases} \tag{6}$$

where $r_1 = g_m m_1$ and $r_0 = g_m m_0$.

Due to the advantages of current mode electronic circuits also the progress in the design of transconductance (G_m), the proposed block diagrams for both Chua's diode as well as Chua's circuit is based on the G_m–C integrators. Three current integrators are shown in Fig. 2 where the following relations are obtained:

$$C_1\dot{V}_X = I_1, \quad I_X = g_{m1}V_X \tag{7a}$$

$$C_2\dot{V}_Y = I_2, \quad I_Y = g_{m2}V_Y \tag{7b}$$

$$C_3\dot{V}_Z = I_3, \quad I_Z = g_{m3}V_Z \tag{7c}$$

By comparing the previous equations with Eq. (5), assuming that $C_1 = C/\alpha$, $C_2 = C$, $C_3 = C/\beta$ and $g_{m1} = g_{m2} = g_{m3} = g_m$. The following relations were obtained:

$$\begin{aligned} I_1 &= I_Y - I_N \\ I_2 &= I_X - I_Y + I_Z \\ I_3 &= -I_Y \end{aligned} \tag{8}$$

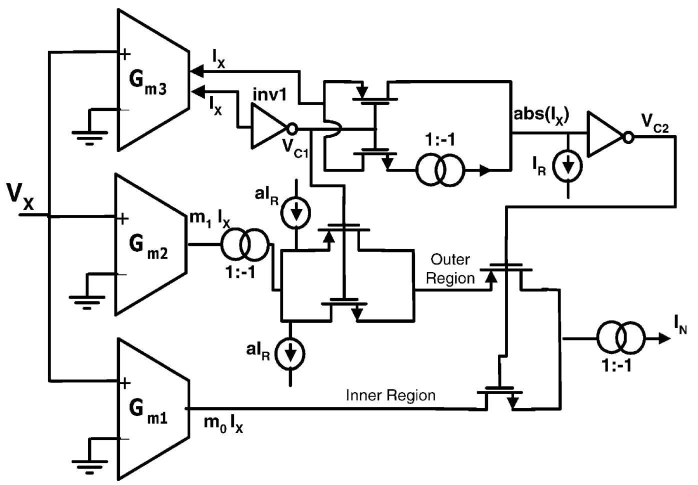

Fig. 3. The general block diagram of the controllable Chua's diode.

It is clear that the relationships are very easy (adding or subtracting) which make it simple to implement by short circuit or current mirrors, where I_N is modeled as follows:

$$I_N = f(V_X) = \begin{cases} m_1 I_X + \gamma I_R, & I_X \leqslant -I_R \\ m_0 I_X, & -I_R < I_X < I_R \\ m_1 I_X - \gamma I_R, & I_R \leqslant I_X \end{cases} \quad (9)$$

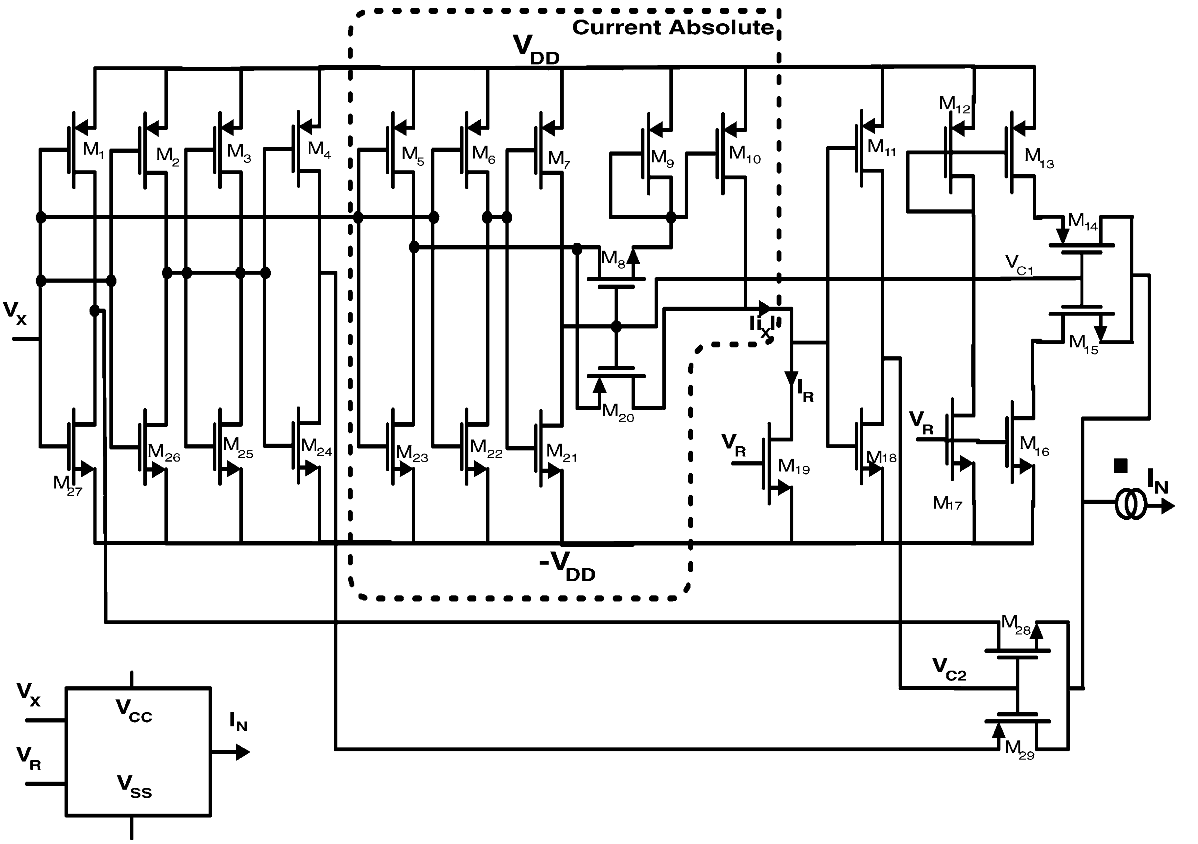

Fig. 4. The MOS circuit realization of proposed Chua's diode.

Table 1
The transistor aspect ratios of controllable Chua's diode circuit

Transistor	Aspect ratio (W/L) (μm/μm)
M_1	10/15
M_2	20/15
M_3, M_4	40/15
M_5, M_6, M_7, M_9, M_{10}, M_{11}, M_{12}, M_{13}	70/15
M_8, M_{15}, M_{28}	50/5
M_{14}, M_{20}, M_{29}	50/1
M_{18}, M_{21}, M_{22}, M_{23}	70/65.5
M_{27}	10/65.5
M_{26}	20/65.5
M_{24}, M_{25}	40/65.5
M_{16}	27/65.5
M_{17}	27/60
M_{19}	63/65.5

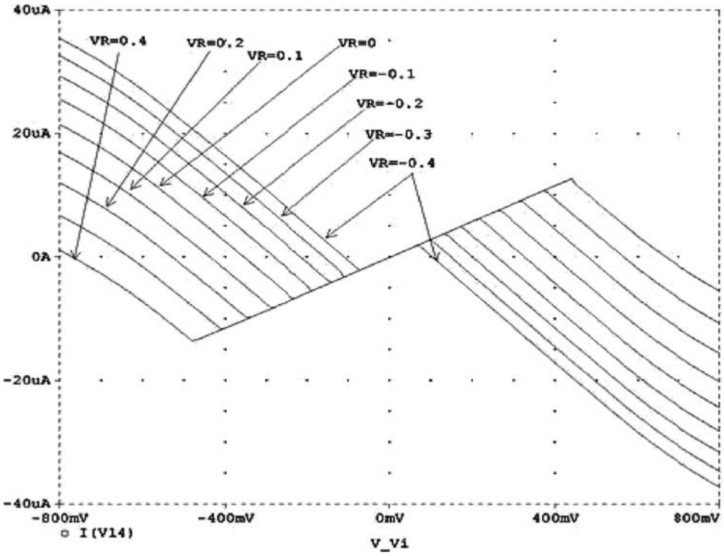

Fig. 5. I_0–V_X projection of Chua's diode with different values of V_R.

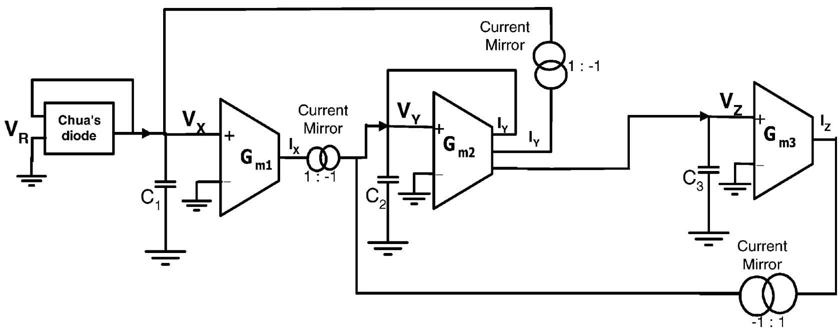

Fig. 6. The proposed block diagram of Chua's circuit.

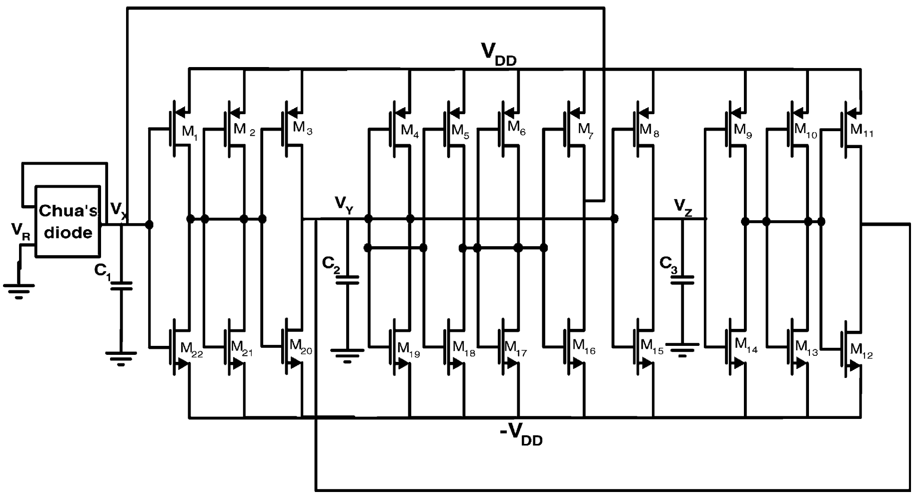

Fig. 7. The complete MOS circuit realization of Chua's circuit.

where $\gamma = (m_1 - m_0)$ is a real constant and $I_R = g_m V_R$ (the reference current).

From the above equations it is clear that the realization of Chua's circuit is dependent on the realization of Chua's diode (I_N).

3. Circuit implementation

The design of Chua's diode is straight forward from Eq. (9) which can be divided into two regions the inner region when the absolute value of I_X is less than I_R with slope of r_0 and the two outer regions with slope of r_1. The outer regions

Table 2
The transistor aspect ratios of Chua's circuit

Transistor	Aspect ratio (W/L) (μm/μm)
M_1, M_2, M_3, M_4, M_5, M_6, M_7, M_8, M_9, M_{10}, M_{11}	70/15
M_{12}, M_{13}, M_{14}, M_{15}, M_{16}, M_{17}, M_{18}, M_{19}, M_{20}, M_{21}, M_{22}	70/65.5

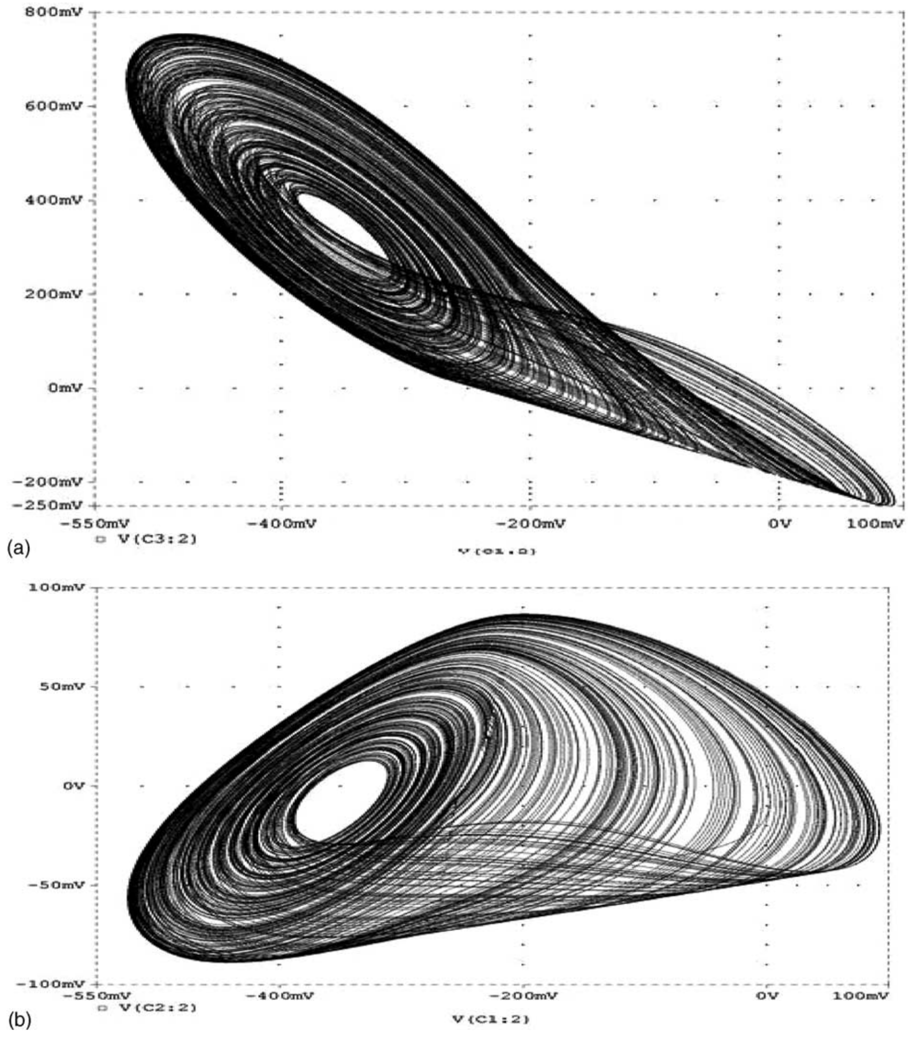

Fig. 8. (a) V_{C1}–V_{C3} projection of Chua's circuit (Rossler type) and (b) V_{C1}–V_{C2} projection of Chua's circuit (Rossler type).

must have an offset current $\pm\gamma I_R$ as a DC value. We can distinguish between the two outer regions by the polarity of I_X (direction of I_X).

Fig. 3 shows the proposed block diagram of Chua's diode. This block diagram consists of three transconductors, six switches and three current mirrors. V_{C1} make a decision for the direction of I_X and controls the first two switches then according to the direction the overall current I_{X1} chooses if the current must be mirrored or kept in its direction. So I_{X1} is the absolute value of I_X. Comparison between I_{X1} and the reference current I_R is performed by the second inverter whose output is V_{C2} to distinguish between the inner and the outer region. The second transconductor achieves the outer region's gain then uses the current mirror due to the negative value of m_1 followed by a DC offset current which discriminate between the two outer regions through V_{C1}. The second comparator output V_{C2} makes a distinction between the inner and outer regions to get I_h then mirrored due to the current direction of the transconductance to obtain I_N.

The main advantages of the proposed block diagram is the exact representation of Chua's diode equation not any approximation and without neglecting the nonlinear part as in [3], also through controlling I_R the breakpoints are changed, which can manage the attractor area through the transition from one region to another.

The typical transconductor [10] (only two transistors such as M_1 and M_{25} in Fig. 3) was used to implement the proposed block diagram. Its transconductance value is given by

$$g_m = 2K(V_{DD} - V_T) \tag{10}$$

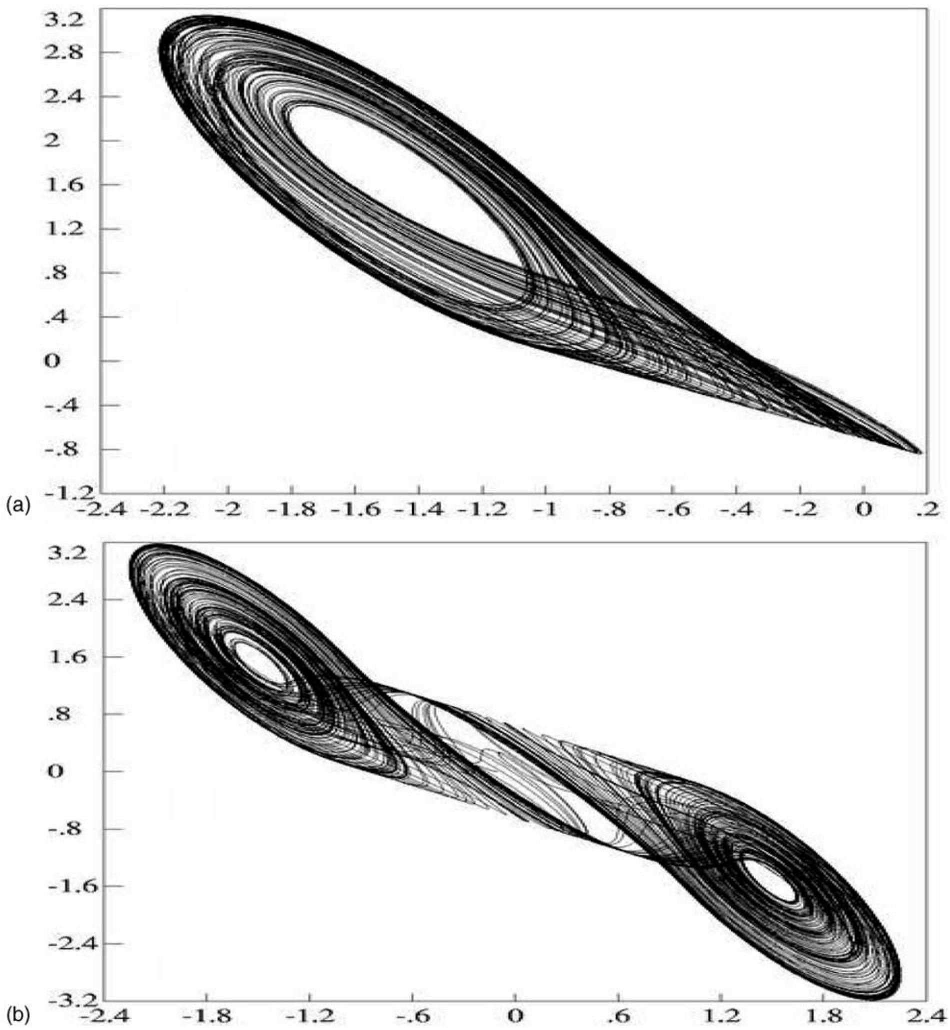

Fig. 9. (a) X–Z numerical projection of Rossler attractor and (b) X–Z numerical projection of the double scroll attractor.

where $K = k(W/L)$, k is the process conductance parameter, (W/L) is the transistor aspect ratio. V_T is the threshold voltage of the transistors [10]. This relation is obtained assuming balanced supply voltage and approximately equal threshold voltages. The aspect ratio of the transistors is designed to ensure that the input voltage of the transconductor is in the proper range.

The circuit implementation of Chua's diode is shown in Fig. 4, the circuit operates on low supply voltage ±1.5 V fulfilling the requirement of portable devices. The reference current I_R is achieved through M_{19} using a reference voltage V_R, also the dependent currents $\pm\gamma I_R$ are achieved by M_{12}, M_{13}, M_{16} and M_{17} using the same reference voltage. The horizontal transistors shown in the realization act as switches. Through the use of V_R we can control the breakpoints of Chua's diode so its possible to control the diode, its block diagram is shown in the same figure.

The transistor-level PSpice simulation of Chua's diode is performed using 0.5 μm Mietec technology. The transistor aspect ratios are listed in Table 1. The output current I_N–V_X projection is shown in Fig. 5 with different values of the reference voltage V_R from −0.4 to 0.4 step 0.1 to show its ability to control the breakpoints of the graph.

The complete proposed block diagram of Chua's circuit is shown in Fig. 6, which uses the symbolic representation of Chua's diode circuit with $V_R = 0$. In addition to Chua's diode, three G_m–C integrators and three simple current mirrors are used. By changing the value of C_1 which already affect the values of the parameters α in Eq. (2) the chaotic behavior

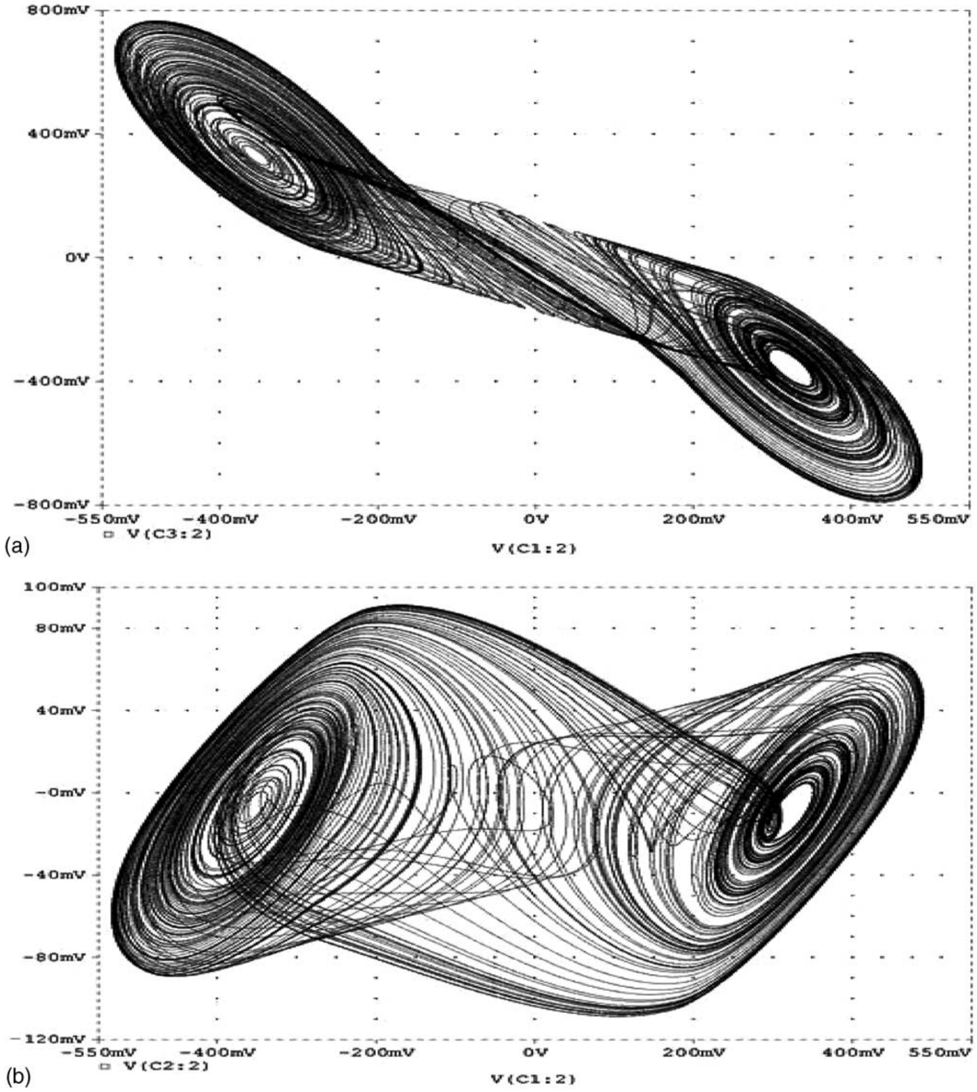

Fig. 10. (a) V_{C1}–V_{C3} projection of Chua's circuit (double-scroll type) and (b) V_{C1}–V_{C2} projection of Chua's circuit (double-scroll type).

will change, for example if $\alpha = 8.5$ Rossler attractor will be obtained and if $\alpha = 9$ the double-scroll attractor is achieved. The other parameter values are the same, where $m_0 = -1/7$, $m_1 = 2/7$ and $\beta = 14$ [2]. The changing of V_R will change the equilibrium points of the attractors.

4. Simulation results

Transistor-level realization is shown in Fig. 7, which operates from a supply voltage of ±1.5 V using the typical transconductor as the G_m block where the values of $C_2 = C = 14$ nF and $C_3 = 1$ nF. The transistor aspect ratios are listed in Table 2. The PSpice simulation using 0.5 μm Mietec technology is performed for both the Rossler attractor and the double scroll attractor.

Rossler attractor is obtained when $C_1 = 1.65$ nF. Fig. 8(a) and (b) shows the V_{C1}–V_{C3} and V_{C1}–V_{C2} projections of the proposed Rossler attractor.

The mathematical numerical solutions of the Chua dimensionless form shown in Eqs. (3) and (4) using fourth order Runge–Kutta method are obtained for both cases when $\beta = 14$, $\alpha = 8.5$ which gives the Rossler attractor and when

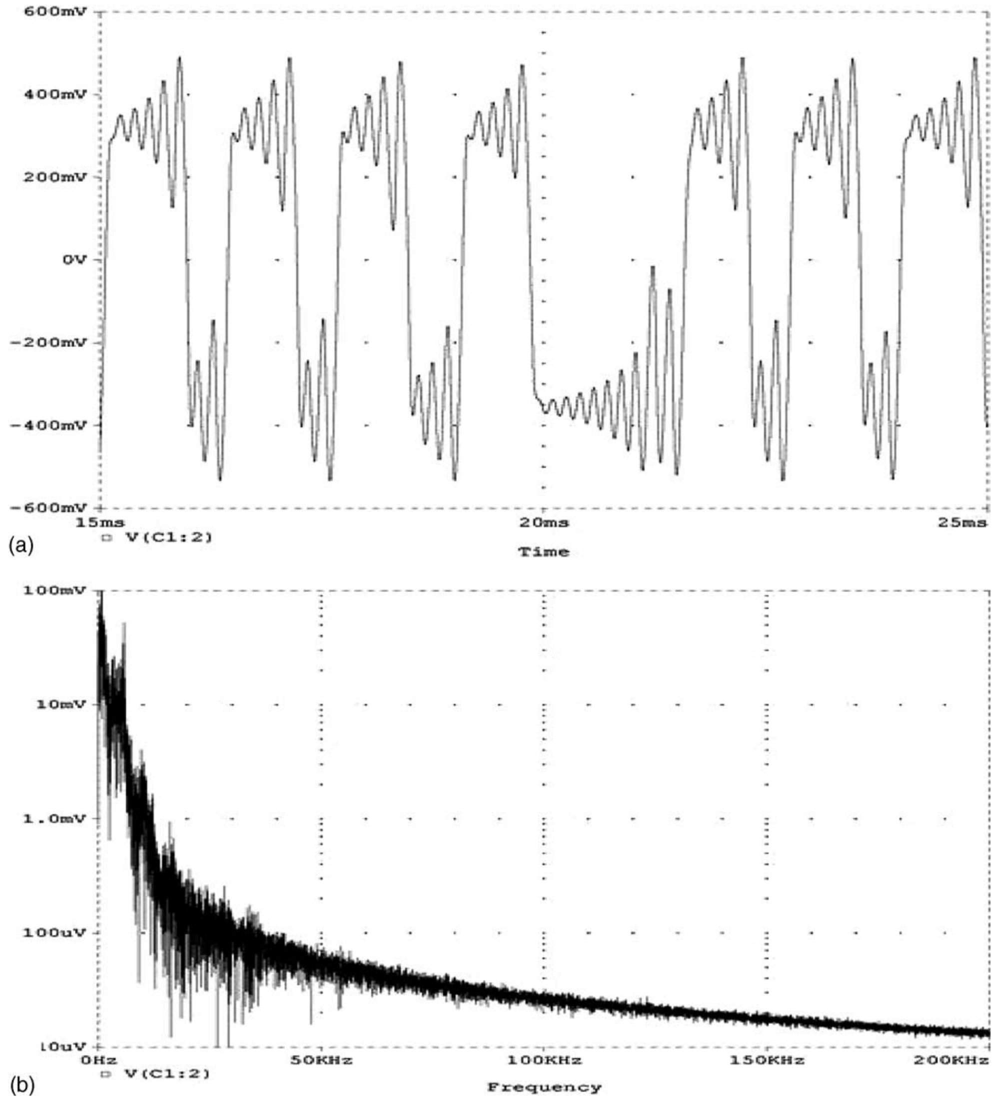

Fig. 11. (a) V_{C1} time waveform of Chua's circuit (double-scroll type) and (b) the frequency response of V_{C1} (double-scroll type).

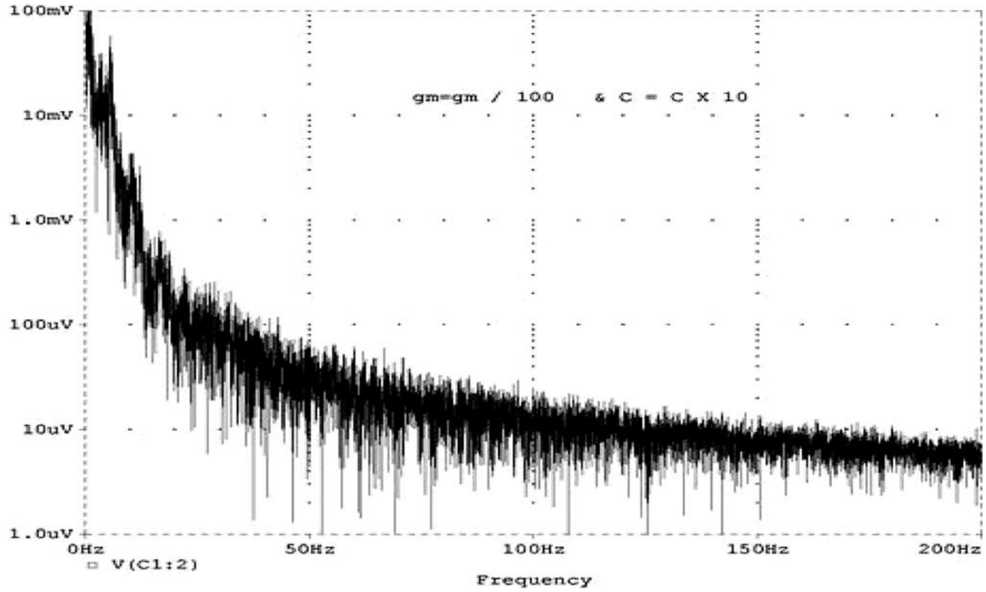

Fig. 12. The frequency response of V_{C1} (double-scroll type) scaled by 0.001.

$\beta = 14$, $\alpha = 9$ which gives the double scroll attractor. Fig. 9(a) shows X–Z projection of Rossler attractor ($\alpha = 8.5$) whereas Fig. 9(b) shows X–Z projection of the double scroll attractor ($\alpha = 9$).

Double scroll attractor is obtained when $C_1 = 1.55$ nF. V_{C1}–V_{C3} and V_{C1}–V_{C2} projections of the double scroll attractor are shown in Fig. 10(a) and (b) while the V_{C1} time waveform and frequency response are shown in Fig. 11(a) and (b).

The proposed circuit can operate over a wide range of frequencies from few Hz to several hundred MHz through changing g_m or C. To slow down the frequency ranges one may decrease g_m or increase C or both as shown in Fig. 12, by decreasing g_m to 0.01 g_m and increasing C to 10 C we scale the frequency ranges of the double scroll attractor to 0.001 of the previous values.

5. Conclusion

G_m–C block diagrams for both the Chua diode in addition to Chua's complete circuit have been introduced. Also new realization for Chua diode at the transistor level and controlled by voltage V_R, which can stretch or contract the inner region of Chua diode by varying the breakpoints of the Chua diode. Rossler attractor and the double scroll attractor can be driven from the proposed complete Chua circuit by changing a single capacitor's value. The proposed circuit operates from low supply voltages as low as ± 1.5 V.

References

[1] Matsumoto T, Chua LO, Komuro GM. The double scroll. IEEE Trans Circ Syst—I 1985;32:798.

[2] Deregel P. Chua's canonical circuit. Electronics research laboratory, College of Engineering, University of California, Berkeley, 1992.

[3] Rodriguez-Vazques A, Delgado-Restituto M. CMOS design of chaotic oscillators using state variables: a monolithic Chua's circuit. IEEE Trans Circ Syst—II 1993;40:596.

[4] Delgado-Restituto M, Rodriguez-Vazques A. Design consideration for integrated continuous-time chaotic oscillators. IEEE Trans Circ Syst—I 1998;45:481.

[5] Delgado-Restituto M, Rodriguez-Vazques A. Integrated chaos generators. In: Proceedings of IEEE. 2002.

[6] Antoniou A. Realization of gyrators using opamps and their use in RC-active network synthesis. In: Proc. IEE. 1969;11:1838.

[7] Torres LAB, Aguirre LA. Inductorless Chua's circuit. Electron Lett 2000;36:1915.

[8] Kennedy MP. Robust Op-amp realization of Chua's circuit. Frequenz 1992;46:66.

[9] Elwakil AS, Kennedy MP. Chua's circuit decomposition: a systematic design approach for chaotic oscillators. J Franklin Inst 2000:251.

[10] Sedra AS, Smith KC. Microelectronic circuits. New York: Oxford University Press, Inc; 1998.